Al-Azhar University Journal
for Medical and Virus Research
and Studies

Comparative Histological Study of The Structure of Mitochondria, in Cardiac Muscle and Proximal Convoluted Tubules of Adult and Senile Male Albino Rats

Rania M. Al Nabawy[1], Mervat Sh. Mehanna[1], Mona H. Hamouda[1], and Fatma S. Abdel Aal[1]

[1]Department of Histology, Faculty of Medicine for Girls, Al-Azhar University, Cairo, Egypt.

***E-mail: raniahisto@azhar.edu.eg**

Abstract

Mitochondria are the main source of Adenosine Triphosphate (ATP) in the cell and play a pivotal role in cell life and death. The heart possesses the highest content of mitochondria of any tissue. The greatest density of mitochondria in the kidney is found in the proximal convoluted tubules (PCTs) and the thick ascending limb of loop of Henle. This work aims to compare the histological structure and distribution of mitochondria in cardiac muscle and PCTs of adult and senile male albino rats. Sixteen male albino rats equally classified into four groups: (GI) Adult male cardiac group, (GII) senile male cardiac group, (GIII) Adult male kidney group and (GIV) senile male kidney group. The selected organs were processed for both light microscopic and Transmission electron microscopic (TEM) examinations using H&E, iron hematoxylin stain, uranyl acetate with lead citrate and immuno-histochemical staining technique utilizing Bcl-2 (B cell lymphoma 2) proteins. Morphometric and statistical analysis for the data were done. H&E stained sections showed general histological structure. Iron HX stained sections showed mitochondria as dark multiple small dots or granules. The highest number of mitochondria was detected in (GII) and the lowest number was detected in (GIV). As regards Bcl-2, the highest area percentage was detected in (GII) and the lowest percentage was detected in (GIV). Ultrastructure features for mitochondria based of TEM. The largest size of mitochondria was detected in (GIII). There was reduction in mitochondrial size in aged cardiac muscle and PCTs. The number of mitochondria increased with senility in aged heart but decreased in aged PCTs. Aged mitochondria expressed disorganization of mitochondrial shape and exhibited different types of structural abnormalities.

Keywords: Mitochondria, Cardiac muscle, PCT, Bcl-2, TEM.

1. Introduction

Mitochondria are essential intracellular double membrane-bound organelles. They are the main source of ATP in the cell and play a pivotal role in cell life and death [1, 2]. Mitochondria generate energy via oxidative phosphorylation and contribute

to the metabolism of nucleotides, amino acids, lipids, and co-factors. They also regulate calcium homeostasis and cellular stress responses [3]. The number and functions of mitochondria vary depending on age, sex, organ, and physiological or pathological conditions [4]. Their number per cell generally reflects the energy demands of that cell [5, 1]. The heart, being the most metabolically active organ in the body, possesses the highest content of mitochondria of any tissue [6] and comprising about 25% of cell volume in human myocardium [7]. The kidneys produce approximately 160–170 L of ultrafiltrate per day. The proximal convoluted tubules contribute to fluid, electrolyte, and nutrient homeostasis by reabsorbing approximately 60 – 70 % of the water and NaCl, a greater proportion of the $NaHCO_3$, and nearly all of the nutrients in the ultrafiltrate. The proximal convoluted tubules are also the site of active solute secretion, hormone production, and many of the metabolic functions of the kidney [8, 9]. The greatest density of mitochondria in the kidney is found in the proximal convoluted tubules and the thick ascending limb [10]. Ageing is characterized by a gradual decline of the functioning of all body systems, with deterioration of cellular ability to proliferate and maintain homeostasis. Ageing-associated dysregulation of the immune system stimulates the production of pro-inflammatory cytokines even when typical inflammation triggers are not present [11]. Several lines of evidence indicate the impact of mitochondria in lifespan determination and ageing [12]. This paper aims to compare the histological structure and distribution of mitochondria in cardiac muscle and proximal convoluted tubules of adult and senile male albino rats.

2. Patients and Methods

2.1 Materials:

Sixteen apparently healthy male albino rats of Wistar strain were used in the present study. They were housed in the animal house at the faculty of medicine for girls, Al-Azhar University. They were allowed to use water and ordinary rat chow ad libitum and were kept under observation for about 7 days for acclimatization.

2.2 Methods:

The animals were divided into four groups, four rats in each . I. Cardiac groups including GI (Adult male cardiac group) & GII (Senile male cardiac group). II. Kidney groups including: GIII (Adult male kidney group) & GIV (Senile male kidney group).

- Adult rats were about 3 months old and were weighing 150–170 gm.
- Senile rats were about 24 months old and weighed 250-300 gm.

The animals were anaesthetized by either inhalation. Ventral middle incision was made, both kidneys were exposed, and the right kidney was extracted, then the heart was removed, washed in saline and cardiac muscle specimens were obtained from the left ventricles of the heart. The samples were fixed by immersion in 10% formalin for (48) hours, then processed for light microscopic examination [13, 14]. The consecutive slides obtained were stained with the following methods: 1. Hematoxylin and Eosin stain (H& E), for studying the general structure [15, 16]. 2. Iron hematoxylin stain, for studying mitochondria [17]. Immunohistochemical techniques use anti-apoptotic Bcl-2 proteins that reside on the outer mitochondrial membrane [18, 19]. For electron microscopic study, the specimens were obtained with special care while the animals were still alive under either inhalation anesthesia. The left kidney was excised, and then carefully cardiac muscles were dissected from left ventricle. The samples immediately were trimmed with a sharp razor blade into small pieces (0.5 mm3 thickness) in a Petry dish filled with 5% glutaraldehyde [20, 21]. The specimens were preceded for ultrastructure examination using Toluidine blue, Uranyl acetate & Lead citrate stains[23 ,22] .

2.3 Morphometrical & statistical study:

The Diameter of cardiac muscle fibers in adult and senile cardiac group (GI & GII) for H&E-stained sections were measured on six fields for each group using magnification x400 by light microscopy. The mean values were obtained in micrometers for each specimen for statistical analysis. In cardiac and kidney groups, Iron HX stained sections were examined for number of mitochondria in standard measuring frame in six non overlapping fields and Bcl-2-stained sections were examined for area percentage for Bcl-2 positive cells expression in six non overlapping fields for each group via magnification (x400 - x100) respectively in all studied groups. By using ImageJ program, and in fixed area percentage (300 μm) in electron microscopic images in cardiac and kidney groups, the number of mitochondria was counted on six fields for each group at magnification x3000, and the outer diameter of mitochondria was measured on six fields for each group at magnification x10000 in all studied groups. The diameter was determined by measuring the smallest and the largest diameter in the mitochondria in (μm) and dividing the result by two. The mean and standard deviation were obtained at Excel sheets.

3. Results

Hematoxylin and eosin-stained sections from the heart wall of (GI) revealed longitudinal sections of the myocardium with large central oval vesicular nuclei and acidophilic sarcoplasm, in addition to appearance of transverse sections of cardiac myocytes with centrally located nuclei. Cardiac muscle cells are joined end to end at special junctions called intercalated discs. These appeared as short faint pink lines that transverse the muscle fibers and were perpendicular to the axis of the cell. In (GII) cardiac myocytes showed some separation from each other. Acidophilic homogenous mass and congested dilated blood vessels were also seen in-between some muscle fibers. Lipofuscin pigment is a red-brown pigment that gradually accumulates with age inside cardiac tissue at each pole of the nucleus was also noticed (Fig. 1). By morphometric study, there was increasing in the mean diameter of cardiac muscle fibers (Fig. 9) in (GII) in relation to (GI).

Iron hematoxylin- staind sections revealed mitochondria inside cardiac muscle fibers in (GI & GII) as darkly stained multiple small dots or granules. There was increasing of their number (Figs. 2, 10) in (GII) in relation to (GI) .

Electron microscopic examination of the myocardium of (GI) revealed the cardiac muscle fibers that had light and dark bands due to the organization of the contractile sarcomere units of the myofibrils. Z lines appeared bisecting light bands, while M lines appeared bisecting dark bands. Rows of mitochondria with visible cristae can be detected in between myofibrils. Mitochondria expressed reduction of their size and increasing in their number between myofibrils in (GII) with atrophy of their crista (Figs. 3, 11). Using immunohistochemical stain, moderate positive cytoplasmic reaction for (Bcl-2) marker was detected in the cardiomyocytes in (GI) while strong positive cytoplasmic immunoreaction for (Bcl-2) marker was detected in the cardiomyocytes (Figs. 4, 10) in (GII). Light microscopic examination of sections from the renal cortex of adult male kidney group (GIII) stained with H&E showed renal corpuscle, proximal convoluted tubules (PCT) and distal convoluted tubules (DCT). The renal corpuscle was consisted of glomerulus and surrounded by visceral and parietal layers of Bowman's capsule. The PCT had large diameter with narrow lumen and ill-defined cell boundaries. They were lined with cubical epithelium, with rounded vesicular basal nuclei and prominent nucleolus. The cells of PCT were exhibit apical brush border. The cells in PCTs in (GIV) showing many cytoplasmic vacuolations in addition of atrophy of the brush border, decrease in the height of the cells and

widening of the lumen of most proximal tubules. There was deposition of connective tissue Fibers in the lumen of some tubules, in addition to apical migration of the nuclei in some cells (Fig. 5). Iron hematoxylin-stained sections of the renal cortex revealing mitochondria that appeared in the basal part of the cells of the PCT as dark lines or threads like structure parallel to the long axis of the cells, and perpendicular to the surface resulting in basal striations. Also, they appeared as dark multiple small dots or granules in the apical part of the PCTs. There was reduction of their number (Figs. 6, 10) in (GIV) in relation to (GIII). Electron microscopic examination of kidney section of (GIII) revealed rod shaped elongated mitochondria that were bounded by intact two membranes separated by intermembrane space. Outer mitochondria membrane was smooth and inner mitochondrial membrane was folded due to presence of the visible cristae. There was disordering of mitochondrial arrangement in (GIV) together with a change in shape and decrease in size with reduction of mitochondrial number (Fig. 11) as compared to (GIII). Some maintained their rod shape with regular outer mitochondrial membrane and visible cristae, and some other became rounded. Some mitochondria became swollen with visible reduction in the mitochondrial density. There were distorted cristae, matrix loss and appearance of electron dense granules in the matrix (Fig. 7). Using immunohistochemistry stain, strong positive cytoplasmic reaction for (Bcl-2) marker was detected in the proximal convoluted tubules in (GIII) as brown granules in the cytoplasm, while weak positive cytoplasmic reaction for (Bcl-2) marker (Figs. 8, 10) was detected in the PCTs in (GIV) .

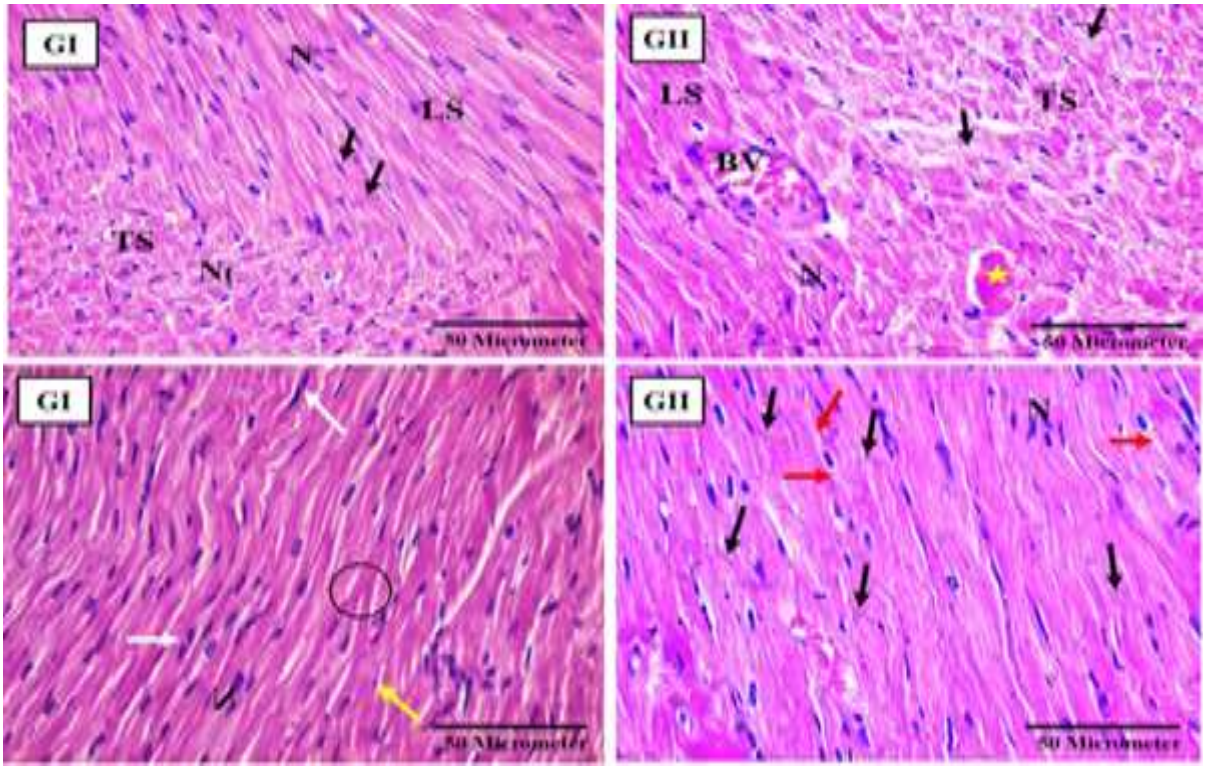

Fig. 1: Photomicrographs of sections in the myocardium revealing longitudinal sections (LS) of the cardiac muscle fibers with central oval nucleus (N), others transverse sections (TS) with central rounded nucleus (Nt) and Intercalated disc (black arrows). Some cardiac myocytes are branched (circle) and some fibers are binucleated (white arrows) with visible spindle shape connective tissue cell (yellow arrow). Cardiac myocytes in (GII) showing some separation of the fibers (black stars), congested blood vessels (BV), acidophilic homogenous mass (yellow star) and lipofuscin pigment (red arrows).(H&E, x400)

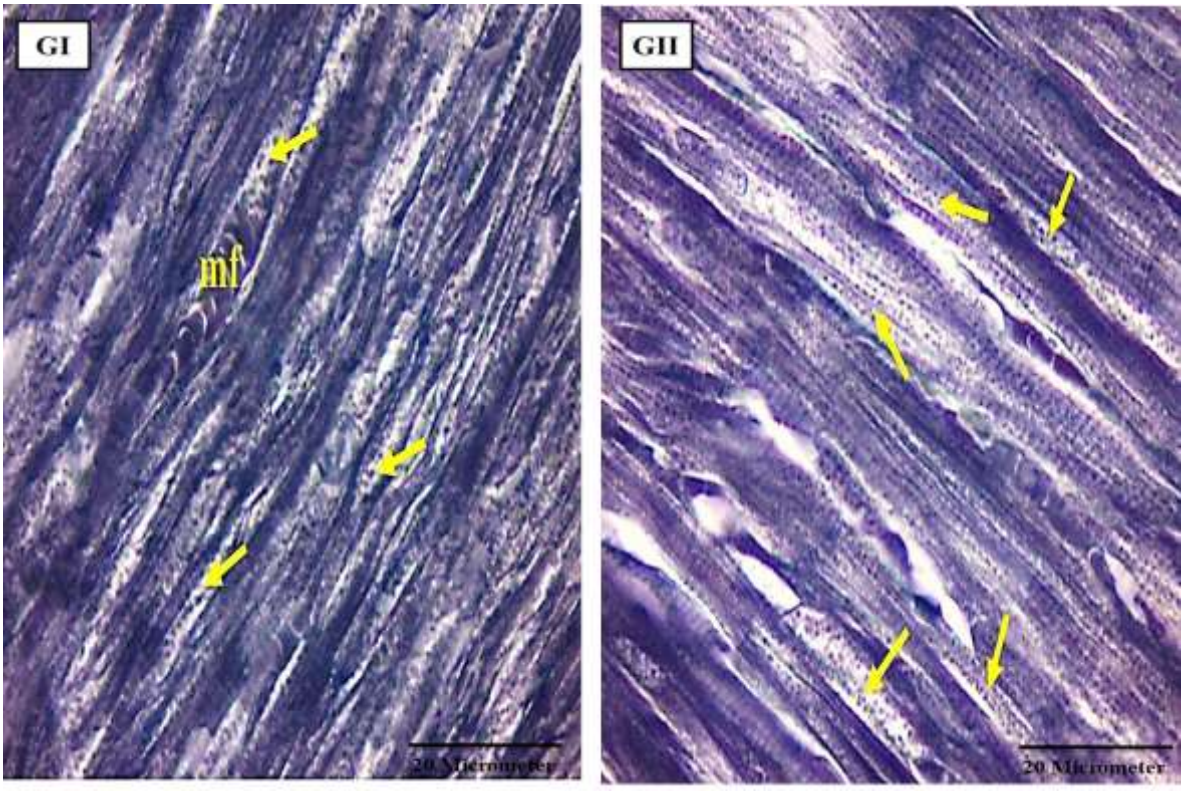

Fig. 2: Photomicrographs of Iron hematoxylin stained sections in the myocardium revealing mitochondria as small dots or granules (yellow arrows) in (GI & GII) with apparent increase of their number in (GII) in relation to (GI).
(Iron hematoxylin, x1000)

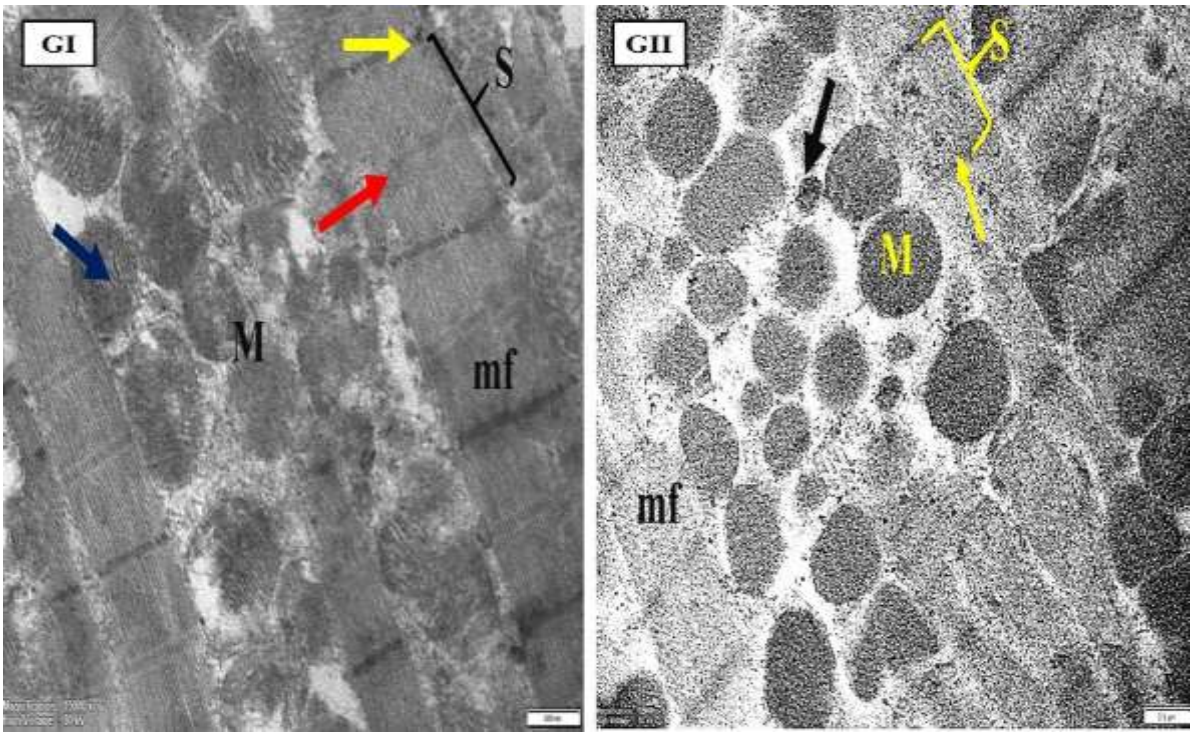

Fig. 3: Electron micrographs of sections in the myocardium showing cardiac myocytes with visible transverse striation of myofibrils (mf) that appeared as parallel longitudinal cylinders between successive Z lines (yellow arrow) bound the sarcomere (S). M lines (red arrows) appear in the middle of the sarcomere. Rows of mitochondria (M) in (GI) are seen in between the myofibrils with visible cristae (blue arrow). More abundant mitochondria (M) with different shapes and size are seen in between the myofibrils in (GII) with more electron dense matrix. Note, small mitochondria in the field (black arrow).(Uranyl acetate and Lead citrate, x15000)

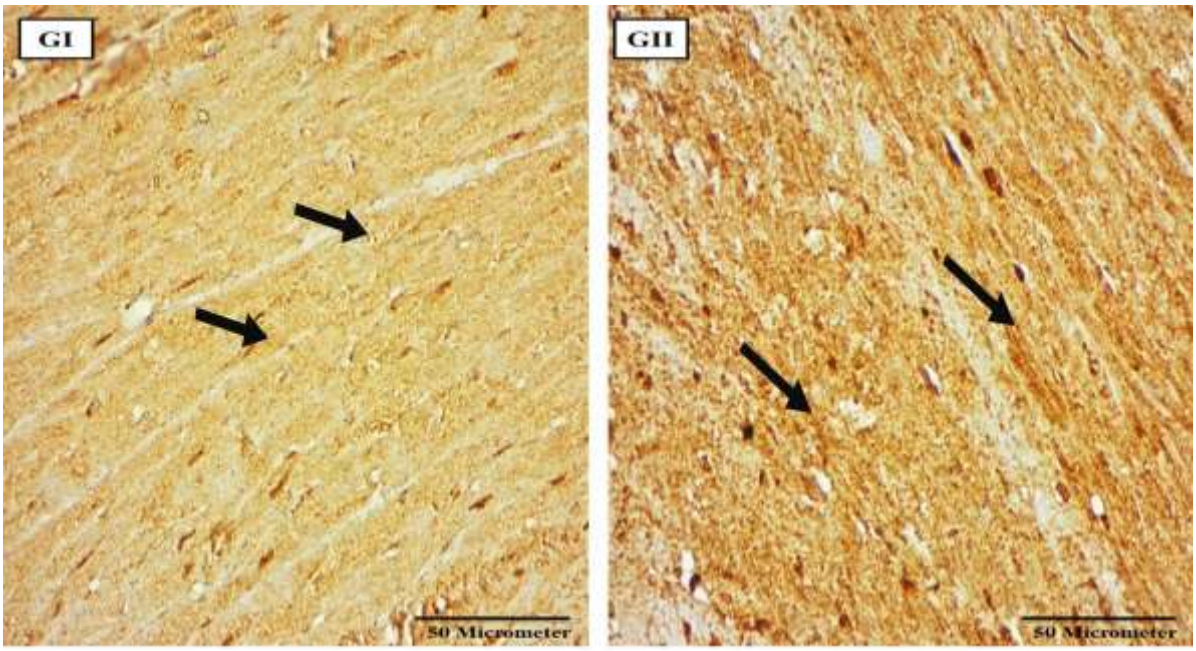

Fig. 4: Photomicrographs of sections in the myocardium revealing: moderate and strong positive (arrows) cytoplasmic immunoreactivity for Bcl-2 in the cardiomyocytes of (GI), and (GII) respectively. (Bcl-2, x400)

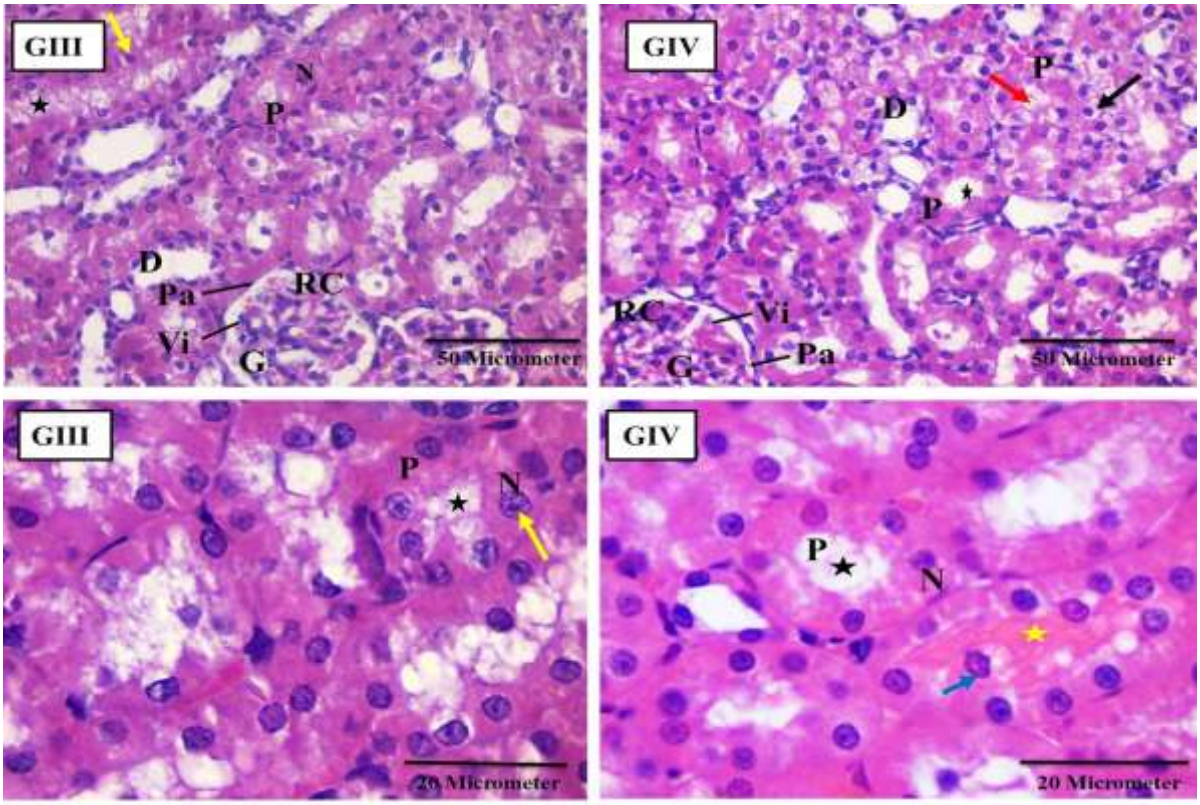

Fig. 5: Photomicrographs of sections in the renal cortex of adult male albino rat kidney group (GIII) revealing renal corpuscle (RC) consisting of glomerulus (G) surrounded by visceral (Vi) and parietal layer (Pa) of Bowman's capsule, PCT (P), distal convoluted tubules (D). The PCT are lined with simple cubical epithelium with rounded nucleus (N), prominent nucleolus (yellow arrows) and visible brush border (black stars). In (GIV), there are multiple focal bare areas (black arrows) with visible apical vacuolation (red arrows). Note, atrophy of the brush border, widening of the lumen in some proximal tubules (black star), apical nuclei in some cells (blue arrow) and deposition of homogenous acidophilic material in the lumen of some tubules (yellow star). (H&E, x400 & x1000)

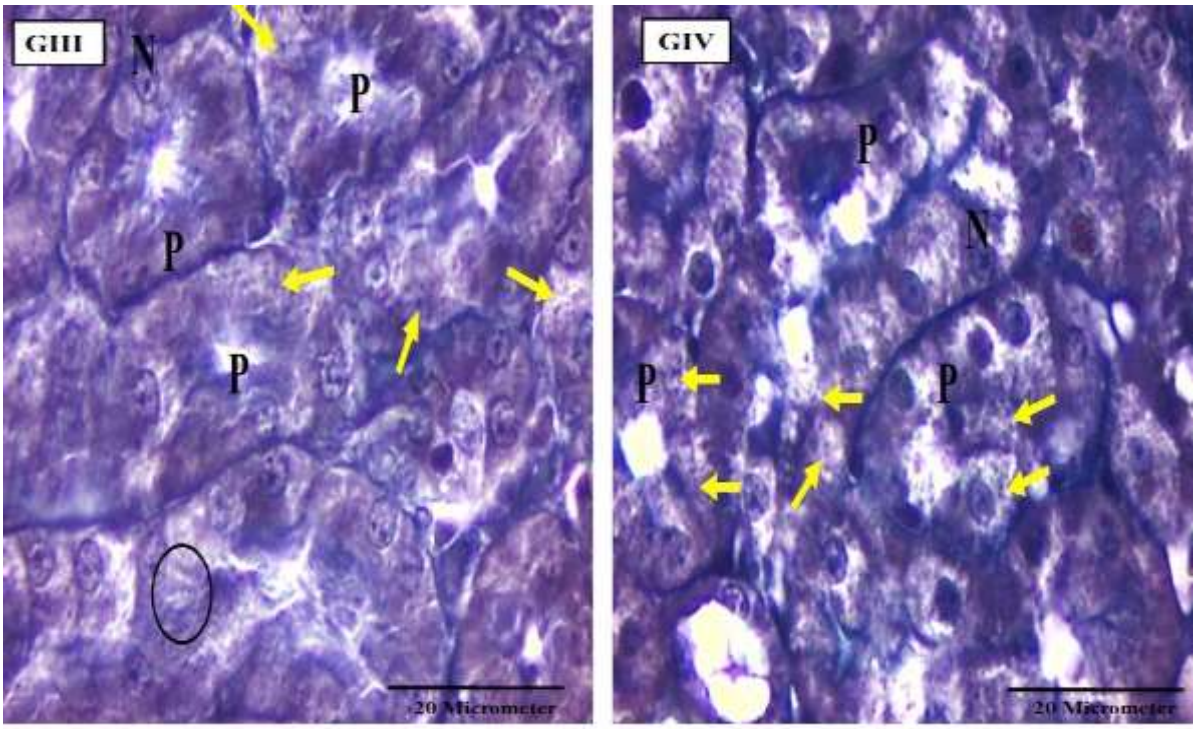

Fig. 6: Photomicrographs of cross sections of renal cortex of adult male albino rat kidney group (GIII) revealing mitochondria that distinguished in the basal part of the cells as dark lines or threads like structure (circles). They appear as dark multiple small dots or granules (yellow arrows) in the apical part of the PCTs. There was apparent decrease of mitochondrial number in (GIV) in relation to (GIII). (Iron hematoxylin, x1000)

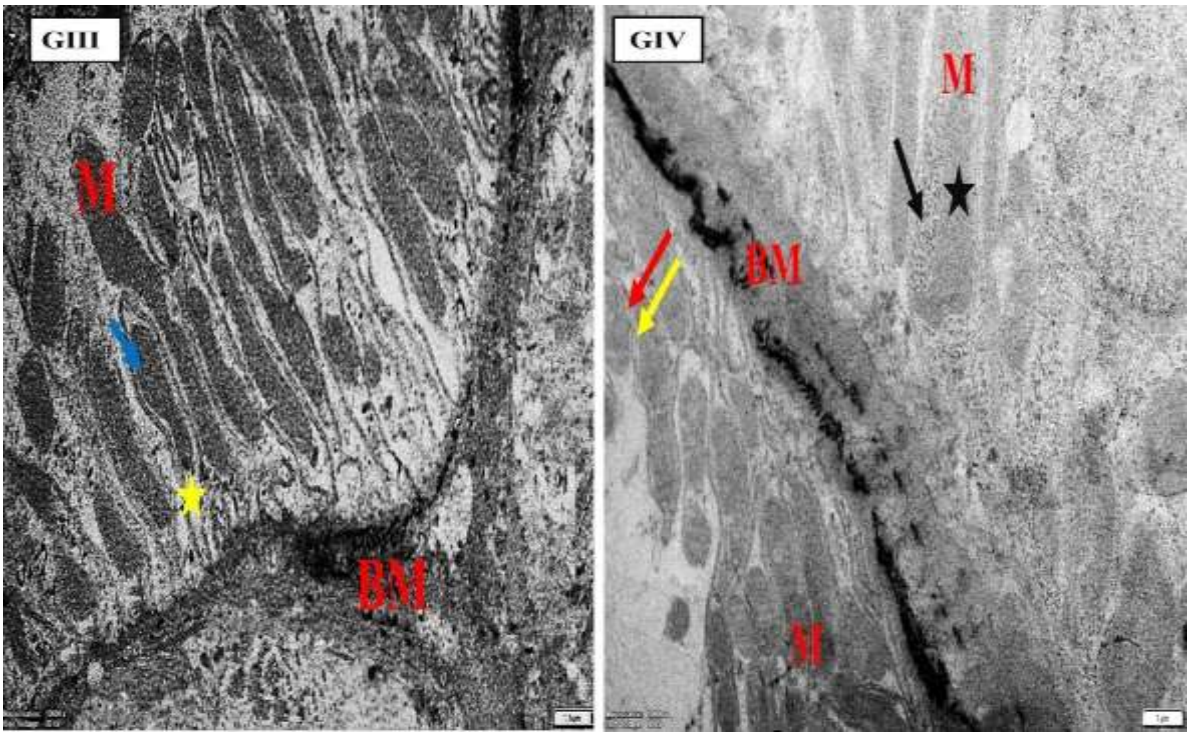

Fig. 7: An electron micrograph of a kidney section of (GIII) revealing that, the cytoplasm of the basal part of PCTs contains numerous closely associated elongated mitochondria (M) with intact cristae (blue arrow) arranged along the basal infoldings that tend to extend deep into the cell (yellow star). Well defined basement membrane (BM) is also illustrated. In (GIV), there are mitochondria with visible outer (red arrow) and inner (yellow arrow) mitochondrial membrane. The mitochondrial density of the matrix is preserved in certain areas (black star) and lost in others which replaced by granular matrix (black arrow). (Uranyl acetate and Lead citrate, x10000)

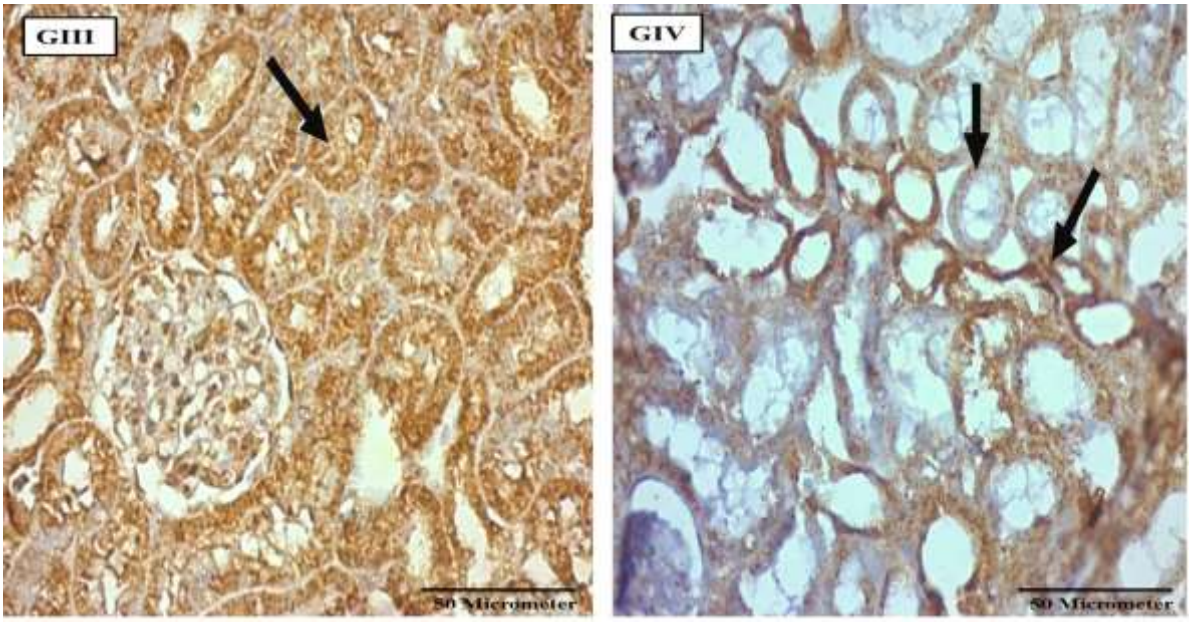

Fig. 8: Photomicrographs of sections in the renal cortex of adult male albino rat kidney group revealing: strong positive cytoplasmic immunoreactivity for Bcl-2 within the cytoplasm of PCTs (black arrows) in (GIII), while weak positive cytoplasmic immunoreactivity for Bcl-2 within the cytoplasm of the PCTs in (GIV). (Bcl-2, x400)

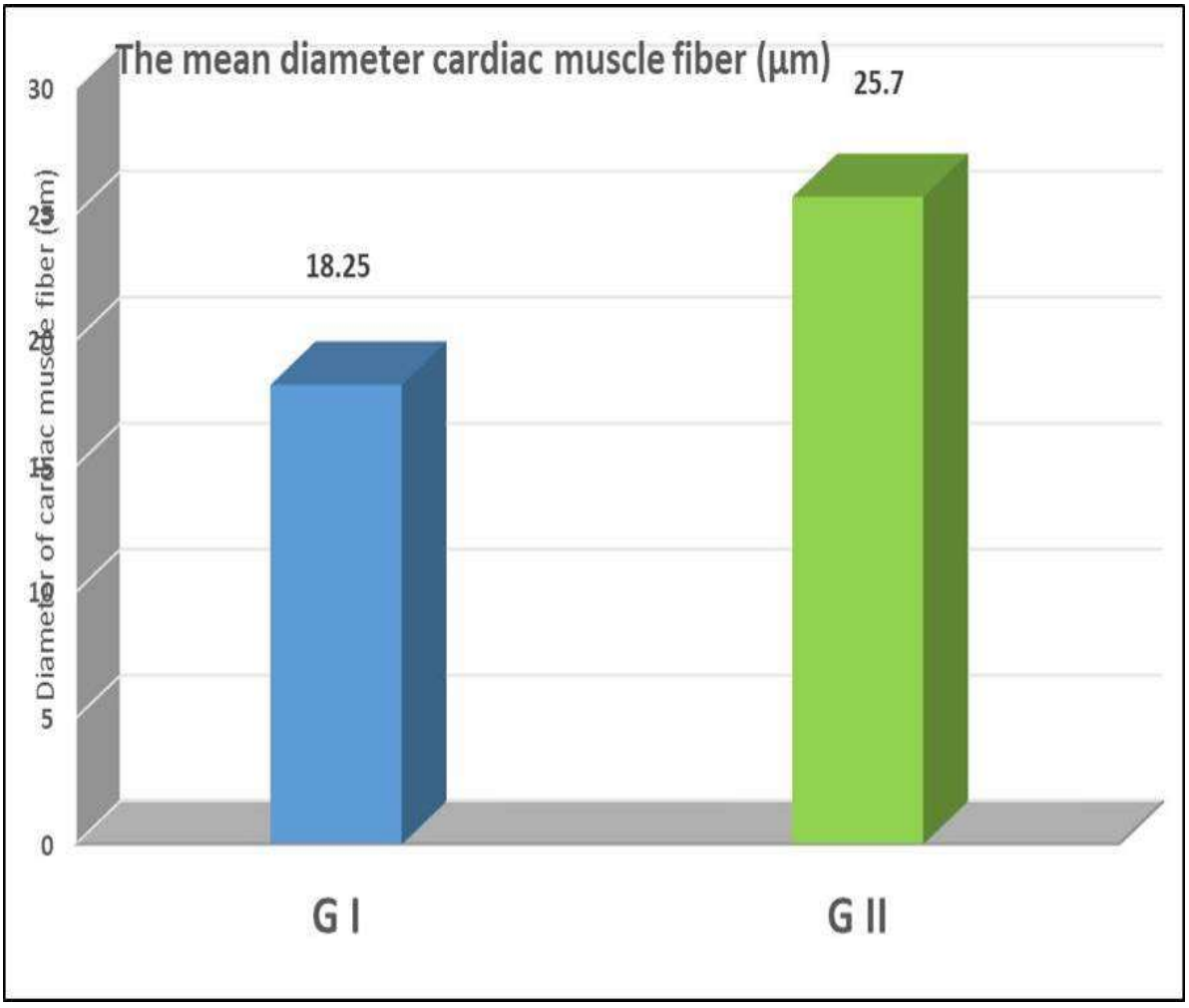

Fig. 9: The mean diameter of cardiac muscle fibers (µm) in adult (GI) and senile (GII) cardiac groups.

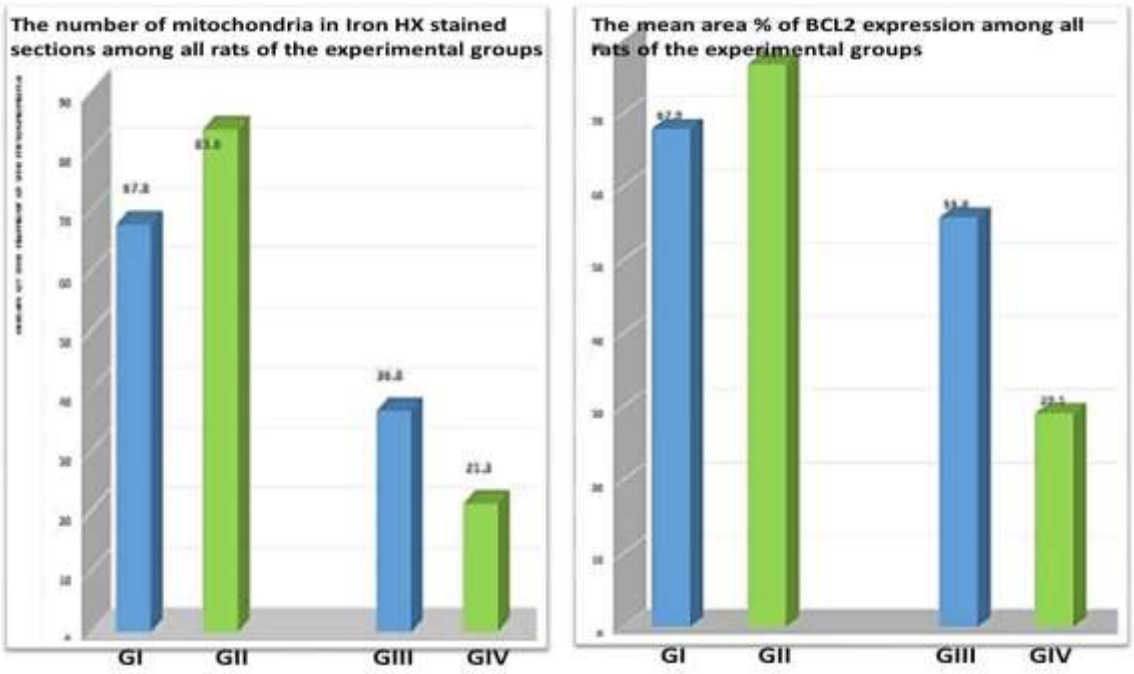

Fig. 10: The mean number of mitochondria in Iron HX stained sections and the mean area percentage of Bcl-2 expression among all rats of the experimental groups.

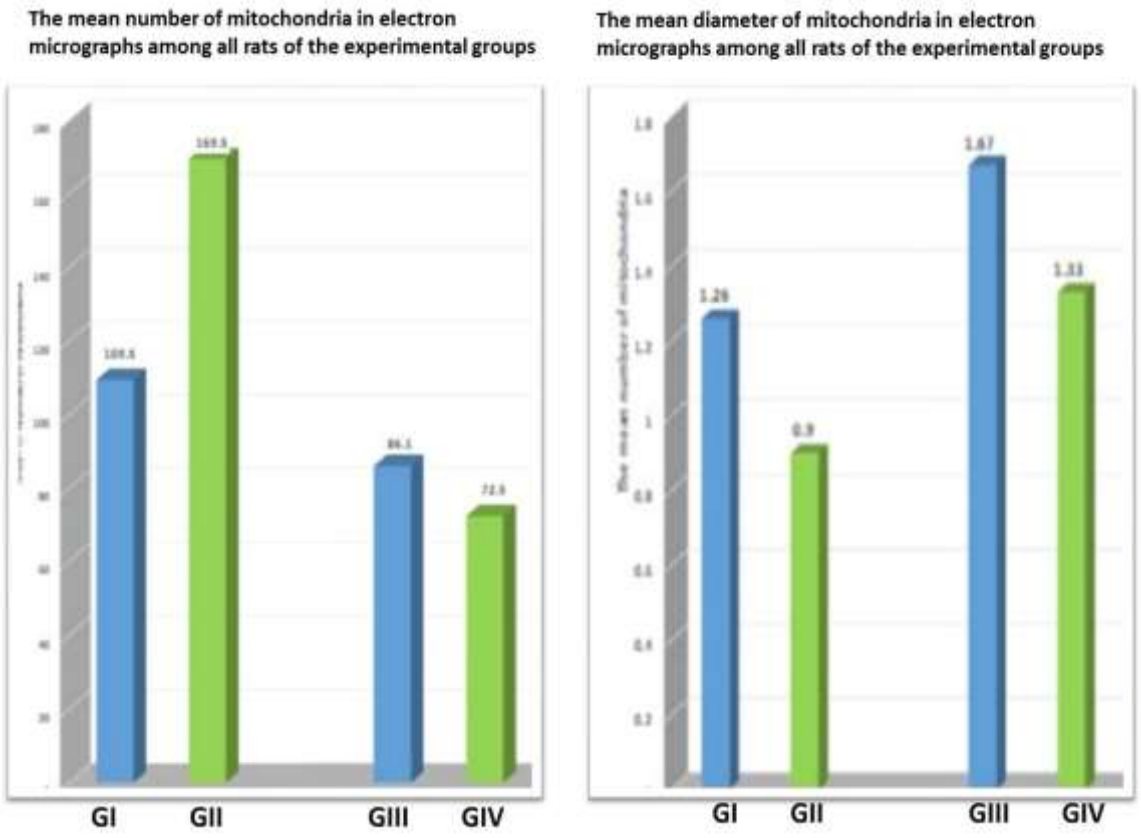

Fig. 11: The mean number and diameter of mitochondria in electron micrographs among all rats of the experimental groups.

4. Discussion

Double Mitochondria have an independent mitochondrial genome (mtDNA) that encodes 13 proteins related to oxidative phosphorylation [24]. We selected the left ventricle to be examined in our practical work because it is subjected to a greater pressure load than the right ventricle because systemic arterial pressure is significantly higher than pulmonary pressure [25]. In H & E-stained sections of the heart wall, there was apparent increase in the thickness of the cardiac wall in (GII) if compared to (G1). This result was supported by Narayana who reported that the cardiovascular system undergoes structural and functional changes over the adult lifespan. With advancing age, the arterial tree becomes stiffer, leading to higher systolic blood pressure and pulse pressure, and a higher risk of systolic hypertension, which predisposes to left ventricular (LV) hypertrophy to maintain a normal left ventricular ejection fraction (LVEF) [26]. Pashkow & Sekar noticed the pyknotic nucleus in the aging heart that might be due to the increased inflammation reaction [27, 25].

In this study, the aging heart also shows lipofuscin pigment that accumulated with ageing inside cardiac tissue at each pole of the nucleus. This was in accordance with Kakimoto who stated that among the whole organs, histological changes in the cardiac tissue are in positive correlation with chronological age, because cardiomyocytes are long-lived cells with limited ability to proliferate after birth. So, he demonstrated for the first time the correlation formula between myocardial lipofuscin accumulation and human chronological age [28]. Cardiac myocytes of (GII) appeared wavy and separated from each other with wide endomysial connective tissue. This was in consonant with the result of Sekar who confirmed these findings by using Masson's trichrome study, showing marked increase in the fibrotic tissue in the aged heart than the adult one [25].

Iron mematoxyline stained histological sections revealed mitochondria as multiple small darkly stained dots inside cardiac muscle fibers. Their number by morphometrical study was higher in (GII) than (GI). This means that the number of mitochondria increasing by aging. These agreed with Hartmut & Johannes who reported that increased mitochondrial number indicating an optimal adaptation for cardiac hypertrophy with ageing [29].

By using immunohistochemistry stain, moderate positive cytoplasmic reaction for (Bcl-2) marker was detected in the cardiomyocytes as brown granules in the cytoplasm in GI, while strong positive cytoplasmic immunoreaction was detected in the cytoplasm in the cardiomyocytes in GII. This means increase in Bcl-2 expression in aging cardiomyocytes. This was explained with Lixin as indicative of a greater level of chronic stress in the old [30].

Bcl-2 proteins are anti-apoptotic/pro-survival members of the B cell lymphoma-2 (Bcl-2) family of proteins that reside on the outer mitochondrial membrane [19]. So, our results suggest increase in the mitochondrial number in aged cardiomyocytes.

Ultrastructure study of mitochondria in (GI) revealed that they were numerous and uniformly distributed in rows separating the myofibrils. They were found oval or elliptical in shape and range in variable sizes. The inner membrane of the mitochondrion gives rise to numerous closely packed cristae that provide an increase in the surface area. The matrix of the mitochondria was moderate electron density and expressed electron dense granules. These were in agreement with Yan who explained that cardiac muscle cells have numerous mitochondria to fulfill the high energy requirements of the cardiac contraction [31]. The mitochondria appeared with different shapes and sizes. There was also increasing in the number of small mitochondria in the myocardium of senile rats. The number of mitochondria

had significantly increased in the myocardium of the senile rats, but the size of mitochondrion was apparently decreased. These were in agreement with Hartmut & Johannes, who decided that age-related alterations of the myocardium are the consequence of an adaptation to an increased load possibly caused by an elevated blood pressure resulting in increased mitochondrial number [29]. Also, Małgorzata confirmed that the numbers of mitochondria in the cardiomyocytes of elderly animals were significantly increased when compared to adult animals [32]. There was atrophy of the mitochondrial cristae in (GII) making them invisible. This supported by Autumn who reported that alterations in mitochondrial structure might be integrally related to the age-related decline in mitochondrial activity [33].

H&E-stained sections of the renal cortex of senile group (GIV) observed various degenerative changes as atrophy of the brush border, and widening of the lumen of most proximal tubules in relation to adult group (GI). There was deposition of connective tissue fibers in the lumen of some tubules. These agreed with Kotob who studied histopathological changes of kidney tissue during aging [34]. Also, there were multiple focal bare areas with visible apical and basal cytoplasmic vacuolations. These were in consonant with Brown who reported that; these vacuolations mainly resulting from apoptotic and degenerative changes in senile proximal convoluted tubules [35]. By morphometrical analysis, the number of mitochondria in Iron hematoxlyine stained sections was more in (GIII) than (GIV). This result was agreed with Tsuneko & Hisashi, who reported that; decrease in the number of mitochondria with aging may be regarded as a similar mechanism to polyploidization of the nucleus, of which division is inhibited [36]. There was strong positive cytoplasmic reaction for (Bcl-2) marker in the proximal convoluted tubules in (GIII). While weak positive cytoplasmic reaction was detected (GIV). Our findings were in agreement with Hyeon who reported that; there was reduction of anti-apoptotic protein, Bcl-2, in the aged rat kidney, this indicates that aged kidney has more apoptotic cells compared to young kidney [37].

Ultrastructural examination of the mitochondria in (GIV) showing that there was disordering of mitochondrial arrangement together with a change in shape and apparent reduction of mitochondrial number as compared to (GIII). These are agreed with Tsuneko & Hisashi [36]. There were distorted cristae, and appearance of electron dense granules in the matrix. These were in agreement with Brandt who reported changes in mitochondrial function and inner membrane structure upon ageing [38].

References

1. Eve Michelle Simcox & Amy Katherine Reeve. (2016): An Introduction to Mitochondria, Their Structure and Functions. Mitochondrial Dysfunction in Neurodegenerative Disorders. 2nd edition. 1, 3-30.

2. Sanyog Jain, Kaisar Raza, Ashish Kumar Agrawal & Ankur Vaidya. (2021): Cell-penetrating peptides in cancer targeting. Nanotechnology Applications for Cancer Chemotherapy. Micro and Nano Technologies. 10; 201-220.

3. Pooja Jadiya & Dhanendra Tomar. (2020): Mitochondrial Protein Quality Control Mechanisms. Genes. 11, 563.

4. Chatterjee, A.; Dasgupta S. & Sidransky, D. (2011): Mitochondrial subversion in cancer. Cancer Prevention Research. 4 (5); 638–654.

5. Acin-Perez, R. & Enriquez, J.A. (2014): The function of the respiratory supercomplexes: the plasticity model. Biochim Biophys Acta. 1837(4); 444–50.

6. David, A. Brown; Justin, B. Perry; Mitchell, E. Allen; Hani, N. Sabbah & et al. (2017): Mitochondrial function as a therapeutic target in heart failure. Nat Rev Cardiol. 14(4); 238–250.

7. Hani N.Sabbah. (2020): Targeting the mitochondria in heart failure: A Translational Perspective. JACC: Basic to Translational Science. 5; 1; 88-106.

8. Norman, P.; Curthoys; Orson, W. & Moe. (2014): Proximal Tubule Function and Response to Acidosis. Clin J Am Soc Nephrol. 9; 1627–1638.

9. Rui Hu & Anita Layton. (2021): Computational model of kidney function in a patient with diabetes. Int. J. Mol. Sci. 22, 5819.

10. Bhargava Pallavi & Rick, G. Schnellmann. (2017): Mitochondrial energetics in the kidney. Nat Rev Nephrol. 13(10); 629–646.

11. Siarhei A. Dabravolski; Varvara A. Orekhova; Mirza S. Baig; Evgeny E. Bezsonov; Antonina V. Starodubova; Tatyana V. Popkova & Alexander N. Orekhov. (2021): The role of mitochondrial mutations and chronic inflammation in diabetes. Int. J. Mol. 22, 6733.

12. Kerstin Boengler; Maik Kosiol; Manuel Mayr; Rainer Schulz & Susanne Rohrbach. (2017): Mitochondria and ageing: role in heart, skeletal muscle and adipose tissue. J Cachexia Sarcopenia Muscle. 8(3); 349–369.

13. Zaghloul, Somaya Saad; Abo-El nour, Rahma Kamal El-din; Abdel Fattah, Marwa Mohamed & Ismail, Dalia Ibrahim. (2019): Comparative histological study on the effect of mesenchymal stem cell and losartan on cardiac injury induced by doxorubicin in male albino rats. 1110-0559(42); 4.

14. Sabry Alaa Abbas; Hytham Mostafa Mohamed; Medhat Mohamed Helmy & Mohamed Ahmed Fouad Elshimy. (2020): laparoscopic mini gastric bypass as a revisional procedure after failed primary restrictive bariatric surgery. 71, 1; 221-235.

15. Bancroft J. & Gamble M. (2015): Theory and Practice of Histological Techniques. 6th ed. Churchill livingstone,Edinburugh, London, Melboure. 201-217.

16. Varun Rastogi; Nikopol Kashyap; Nisha Madhesi; Nishant, Ashwini Dayma & Jyoti Sharma. (2019): Comparison of three alum hematoxylin–harris, mayer's, ehrlich hematoxylin using different tissues–A study of 60 cases. Mod App Dent Oral Health. 2637-4692, 3 (5).

17. Godwin Avwioro. (2011): Histochemical uses of hematoxylin-areview. JPCS.(1). www.arpapress.com/Volumes/JPCS/Vol1/JPCS_1_05.

18. Hewitt, SM; Baskin, D G; Frevert, C W & et al., (2014): Controls for Immunohistochemistry. The Histochemical Society's Standards of Practice for Validation of Immunohistochemical Assays. J Histochem Cytochem., 62(10); 693–697.

19. Jennefer Lindsay; Mauro Degli Esposti & Andrew P. Gilmore. (2011): Bcl-2 proteins and mitochondria--specificity in membrane targeting for death. Biochimica et Biophysica Acta. 1813,532–539

20. Mohamed, Doha S. & Nor-Eldin, Eman K. (2018): Histological and immunohistochemical study of the

possible protective effect of folic acid on the methotrexate- induced cardiac muscle toxicity in male albino rats. Egyptian Journal of Histology. 41, 1; 73-82.

21. Mohamed, Hanan E.; Al-Eryan, Nadia H.; Elsayed, Mohamed F.; Salah-Eldin, Ghada. (2020): Effects of punica granatum peel extract and/ or sitagliptin on induced diabetic nephropathy in adult male albino rats. JRAM 2020. 1 (2): 108 -121.

22. Johanneseen J. (1978): Electron microscopy in humn medicine. Instruments and Techniques. McGraw Holl international book company, New York, San Francisco, London; 1: 20-57.

23. Williams, David B., Carter, C. et al., (1996): Transmission Electron Microscopy A Textbook for Materials Science1st (First) Edition Springer-Verlag New York, LLC: 200-280.

24. Hedong, Lu; Xiaolei, Wang; Min, Li; Dongmei, Ji; Dan, Liang; Chunmei, Liang; Yajing, Liu; Zhiguo, Zhang; Yunxia, Cao & Weiwei, Zou. (2023): Mitochondrial unfolded protein response and integrated stress response as promising therapeutic targets for mitochondrial diseases. Cells. 12(20); 1.

25. Sekar Suresh; Anandan Balakrishnan; Raziya Banu & Seppan Prakash. (2013): Ageing induced changes in ventricular myocardium: A histological and histomophometrical study. International Journal of Anatomical Sciences, 4(2); 03-10.

26. Narayana Sarma V. Singam; Christopher Fine & Jerome L. Fleg. (2020): Cardiac changes associated with vascular aging. Clinical Cardiology. 43; 92–98.

27. Pashkow, FJ. (2011): Oxidative stress and inflammation in heart disease: Do antioxidants have a role in treatment and/or prevention? Int J Inflammation. 514623, 9.

28. Yu Kakimoto; Chisa Okada; Noboru Kawabe; Ayumi Sasaki; Hideo Tsukamoto; Ryoko Nagao & Motoki Osawa. (2019): Myocardial lipofuscin accumulation in ageing and sudden cardiac death. Scientific Reports. 9, 3304.

29. Hartmut Frenzel & JOhannes Feimann. (1984): Age-dependent structural changes in the myocardium of rats. A quantitative light- and electron-microscopic study on the right and left chamber wall. Mechanisms of Ageing and Development. Elsevier Scientific Publishers Ireland Ltd. 27; 29-41.

30. Lixin Liu; Gohar Azhar; Wei Gao; Xiaomin zhang & Jeanne, y. wei. (1998): Bcl-2 and Bax expression in adult rat hearts after coronary occlusion: age-associated differences. Am J Physiol. Jul. 275(1); R315-22.

31. Yan Sun; Seung-Min Lee; Bon-Jin Ku & Myung-Jin Moon. (2020): Fine structure of the intercalated disc and cardiac junctions in the black widow spider Latrodectus mactans. Sun et al. Applied Microscopy. 50:20.

32. Małgorzata Łysek-Gładysin´ska; Anna Wieczorek; Artur Józ´wik; Anna Walaszczyk; Karol Jelonek; Gra˙zyna Szczukiewicz-Markowska; Olaf K. Horban´czuk; Monika Pietrowska; Piotr Widłak & Dorota Gabrys. (2021): Aging-Related Changes in the Ultrastructure of Hepatocytes and Cardiomyocytes of Elderly Mice Are Enhanced in ApoE-Deficient Animals. Cells. 10, 502.

33. Autumn Tocchi; Ellen, K. Quarles; Nathan Basisty; Lemuel

Gitari & Peter, S. Rabinovitch. (2015): Mitochondrial Dysfunction in Cardiac Ageing. Biochim Biophys Acta.; 1847(11); 1424–1433.

34. Kotob Mohamed, H.; Ahmed, M. Hussein & Mahmoud Abd-Elkareem. (2021): Histopathological changes of kidney tissue during aging. SVU-International Journal of Veterinary Sciences. 4(1); 54-65.

35. Brown, C. A.; Elliot, J.C.; Schmiedt, W. & Brown, S. A. (2016): Chronic Kidney Disease in Aged Cats: Clinical Features, Morphology, and Proposed Pathogeneses. Veterinary Pathology. 53(2); 309-326.

36. Tsuneko Sato & Hisashi Tauchi. (1982): Age changes of mitochondria of rat kidney. Mechanisms of Ageing and Development. 20; 111-126.

37. Hyeon Ji Leea; Kyung Jin Junga; Jung Won Kima; Hyon Jeen Kima ; Byung Pal Yub & Hae Young Chunga. (2004): Suppression of apoptosis by calorie restriction in aged kidney. Experimental Gerontology. 39; 1361–1368.

38. Brandt Tobias; Arnaud Mourier; Luke S Tain; Linda Partridge; Nils-Göran Larsson & Werner Kühlbrandt. (2017): Changes of mitochondrial ultrastructure and function during ageing in mice and Drosophila. eLife. 12;6; e24662.